

A POD INVESTIGATION OF THE THREE-DIMENSIONAL WALL JET NEAR FIELD

Lhendup Namgyal

Department of Mechanical Engineering
University of New Brunswick
Fredericton, New Brunswick, Canada
email: q8196@unb.ca

Joseph W. Hall

Department of Mechanical Engineering
University of New Brunswick
Fredericton, New Brunswick, Canada
email:jwhall@unb.ca

ABSTRACT

A turbulent three-dimensional wall jet was investigated at an exit Reynolds number of 2.5×10^5 using Stereoscopic Particle Image Velocimetry (PIV) in the near-field region ($x/D=5$). The Proper Orthogonal Decomposition (POD) was applied to all three components of the velocity field to investigate the underlying coherent structures in the flow. Low-dimensional reconstructions of the turbulent velocity field using the first 5 POD modes showed that the streamwise flow contours are significantly distorted from the mean. This was induced by coherent streamwise vortex structures formed in the outer shear-layers of the wall jet, not unlike those found in free jets. The reconstructed instantaneous streamwise vorticity indicates the presence of a persistent vortex pair close to the wall and on either side of the jet centreline that are similar to the mean streamwise vorticity. These regions do not appear to be directly related to the streamwise vortex structures in the outer shear-layers.

INTRODUCTION

Three-dimensional wall jets are formed when a fluid flows from a finite width opening, tangentially along a wall. Wall jets have a diverse range of engineering applications, such as the cooling of gas turbine combustor walls and in ventilation systems. The most common application of wall jets from daily life is likely the automobile windshield defroster. One of the most noteworthy features of the three-dimensional wall jet is that the lateral spread rate in the far-field is five to eight times greater than the vertical spread rate normal to the wall (Launder and Rodi, 1983; Craft and Launder, 2001; Sun, 2002; Hall and Ewing, 2007a; Namgyal and Hall, 2010). The cause of the large lateral spread rate in three-dimensional wall jets is not fully understood; however, Launder and Rodi (1983) argued that this behaviour was caused by the presence of strong mean secondary flows in the jet.

In order to understand the origin of the secondary flow in a three-dimensional wall jet, the turbulent velocity field is investigated here in the near-field region of the wall jet at $x/D = 5$ using Stereoscopic PIV. The Proper Orthogonal Decomposition (POD) technique, first introduced to the turbulence community by Lumley (1967), is used here to extract the underlying organized motions in the flow field. The POD is a powerful technique for extracting energetically dominant modes in a flow by decomposing a series of data into an optimal set of orthogonal basis functions, and has been used widely for extracting the coherent structures in turbulent flows (Glauser, 1987; Ukeiley et al., 1999; Citriniti and George, 2000; Pinier, 2007; Tinney et al., 2008).

EXPERIMENTAL SETUP

The air flow to the jet was supplied by a 6.5HP, single stage centrifugal blower. The flow is conditioned in a 0.9m x 0.9m x 0.9m settling chamber which has three 10 mm screens. The flow from the settling chamber is then passed through a flow straightener placed inside a 0.20m diameter pipe. Finally, the air flows through a contoured nozzle with an area contraction ratio of 28:1. The nozzle has a fifth order polynomial profile so as to produce a top hat exit velocity profile and less than 0.25% turbulence intensity. The jet Reynolds number at the exit was set to 2.5×10^5 . Upon exiting the nozzle the air flows tangentially along a 2.49 m x 2.08 m horizontal wall forming the three-dimensional wall jet.

The velocity field was acquired using a *LaVision* Stereoscopic PIV system. The flow was seeded using olive oil droplets generated by a Laskin type atomizer. This produced a mean particle diameter of $3\mu\text{m}$. A Solo 120XT Nd-Yag laser having a pulse energy of 120mJ was used to illuminate the flow. The images from the tracer particles were acquired by a pair of 12 bit CCD cameras (*LaVision* Image intense) with a resolution of 1376 x 1040 pixels. The double frame instantana-

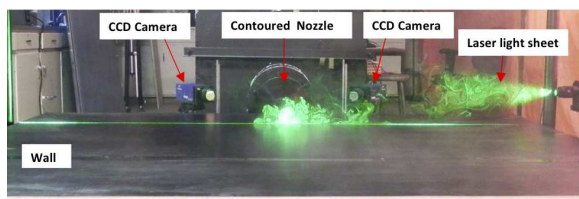


Figure 1. Experimental setup.

neous images were processed using *LaVision Flow Manager (DaVis 7.2 version)*. Multi-pass decreasing interrogation window sizes of 32×32 with 75% overlap were used here along with a normalized correlation function. The processed data was then reconstructed using the Whittaker algorithm.

Both the laser and the cameras were arranged as shown in figure 1. In order to have a statistically converged data, 3000 independent pairs of images were taken at $x/D = 5$. Since every vector field could be considered an independent event due to the time lag between image pairs, the uncertainties in the mean streamwise velocity at the centre of the jet at y_{max} , and $y_{1/2}$ were determined to be 0.14% and 1.12% (19 times out of 20), respectively. Here, x , y and z are the streamwise, normal and lateral coordinates respectively, and D , is the diameter of the nozzle exit.

EXPERIMENTAL RESULTS

The contours of the 3 mean velocity components measured at $x/D = 5$ are shown in figures 2 through 4. In all the cases, the results have been normalized by the local maximum streamwise velocity, \bar{U}_{max} and the jet half-widths. The mean streamwise flow velocity contours are still quite round at this location as expected since the nozzle is round, but there is a slight bulging of the mean contours near the wall. This bulging is associated with the development of outward lateral velocities in the jet, as shown in figure 4. In particular, the lateral velocities in the center of the jet between the lateral shear-layers are directed outward, whereas the lateral velocities outside of the half-widths are directed inward but are slightly further from the wall. Hall and Ewing (2007a,b, 2010) have previously discussed the importance of the lateral shear-layers in the development of three-dimensional wall jets, but did not see this inward lateral entrainment of the flow by the shear-layers. This was likely due to difficulties associated with using hot-wire techniques in regions where strong flow reversals persist.

The contours of the mean velocity normal to the wall, shown in figure 3, are positive in the region between the lateral shear-layers indicating that the jet is on average growing vertically, whereas outside the lateral shear-layers there is a net downward movement of air to supply the aforementioned lateral entrainment of the ambient air. The slight offset of the mean lateral velocities and the rapid change in sign of the causes two regions of counter-rotating vorticity near the wall and on either side of the lateral shear-layers, as shown in figure 5. These results are similar to those noted in the near-field of the three-dimensional wall jet by Matsuda et al. (1990), Sun (2002), and Hall and Ewing (2007a,b, 2010) but are somewhat closer to the wall than previously observed. This may be due to the higher Reynolds number jet used here than in the previous studies, but is likely due to the improved spatial resolu-

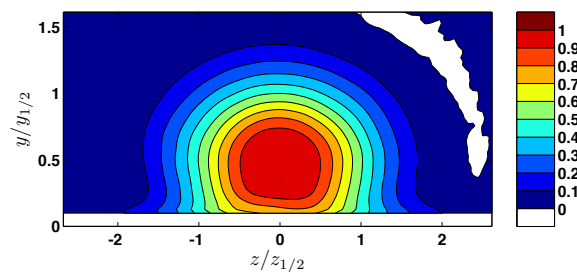


Figure 2. Contours of the normalized mean streamwise velocity.

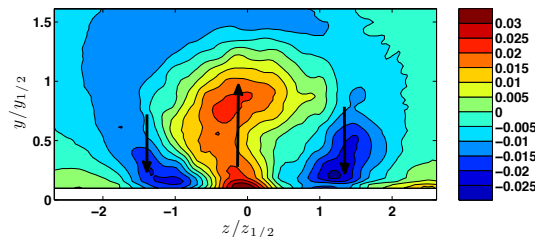


Figure 3. Contours of the normalized mean velocity normal to the wall.

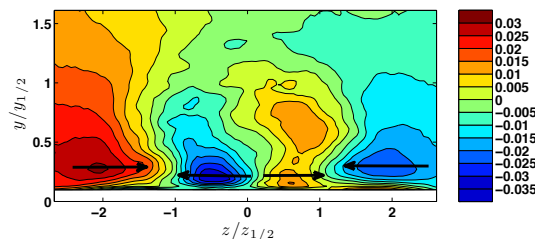


Figure 4. Contours of the normalized mean lateral velocity.

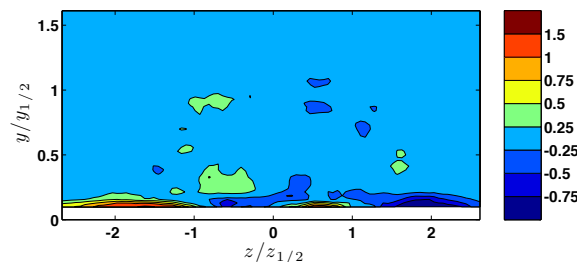


Figure 5. Contours of the mean streamwise vorticity.

tion of the PIV technique used here than the cross-wires used in the previous studies (Matsuda et al., 1990; Sun, 2002; Hall and Ewing, 2007a,b, 2010). Interestingly, the highest value of V occurs along the wall at the jet centerline and is likely associated with rapid development of the wall jets inner layer.

The snapshot POD, as outlined by Sirovich (1987), was applied to the stereoscopic PIV data following the methods described by Meyer et al. (2007). To ensure that the POD

was properly resolved, all 3000 snapshots were used in the POD analysis. Note that this is larger than the number of snapshots used in previous studies; for example, Meyer et al. (2007) found satisfactory results using 1000 snapshots in their analysis of a turbulent jet in cross-flow, whereas Agelinchaab and Tachie (2011) used 1600 snapshots in the symmetry (x - y) and lateral (x - z) planes of a turbulent three-dimensional wall jet. As the wall jet development is not axisymmetric due to the presence of the wall, the POD was applied to the rectilinear grid produced by the PIV system and not an axisymmetric coordinate system as is commonly done on round free jets (Citriniti and George, 2000; Pinier, 2007; Tinney et al., 2008).

The energy associated with each mode and the cumulative energy distribution is shown in figure 6. The first mode accounts for 3.5% of the total turbulent energy. These results are again in line with those of Agelinchaab and Tachie (2011), who captured 2.4% of the total turbulent energy in the first mode in the developing region ($12 \leq x/D \leq 24$) and 16.6% in the self-similar region ($60 \leq x/D \leq 72$). Pinier (2007) performed Dual-time PIV on a compressible round jet formed using a contoured nozzle, and rather than decompose the coordinate system onto an axisymmetric grid, performed the POD on a rectilinear grid; he found that 3.5% of the total turbulent energy was contained in the first mode.

The first 5 POD mode-shapes are shown in figure 7. Here, the contours represent the streamwise velocity component of the mode-shapes, whereas the vector plots illustrate the normal and lateral components. The streamwise velocity component of the first POD mode-shape has two dominant regions with opposite sign located on either side of the jet centreline. This is consistent with the findings of Hall and Ewing (2010, 2007b), who computed the POD of the spanwise fluctuating wall pressure in the near-field of a three-dimensional wall jet and found that the first mode was primarily antisymmetric. The vector plot indicates that the antisymmetry of the streamwise velocity is associated with a strong lateral movement of fluid across the entire span of the jet. Reconstruction of the instantaneous velocity field using only this mode indicates that it is associated with a side to side meandering in the jet, again consistent with the findings of Hall and Ewing (2010).

The contours of the streamwise velocity associated with the second POD mode has 4 regions of oppositely signed velocity. The vector field indicates that these are related to streamwise vortex structures, not unlike those found in the shear-layers of a free jet formed using contoured nozzles (Citriniti and George, 2000; Pinier, 2007; Tinney et al., 2008). In this case, the rotational flow patterns are oriented to induce a strong jet-like inflow of fluid on the upper left side of the flow and an outflow on the top outer right of the jet. Note that these flow patterns would be reversed when the mode-shape becomes negative. The third POD mode-shape is symmetric and the rotational flow is oriented to cause fluid ejections on the upper edges of the jet and an inflow at the bottom of the jet near the wall. The next higher POD mode-shapes are similar but all have an increasing number of lobes. Consistently, in each of the cases, the lobes are accompanied by streamwise vortices.

A low-dimensional reconstruction of the instantaneous velocity field was performed to spatially filter out the small-

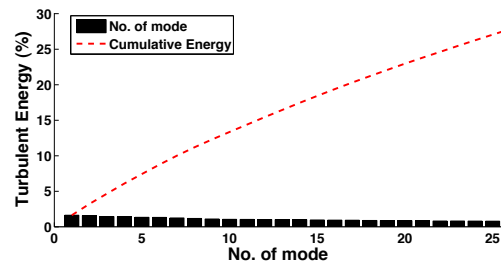


Figure 6. Turbulent energy distribution in the POD modes.

scale structures so that the dynamics of the large-scale structures in the wall jets could be examined. Five POD modes were chosen as a reasonable first attempt at understanding the coherent structures in the jet. Together, the first 5 POD modes capture 15.7% of the total turbulent kinetic energy in the jet. The actual and reconstructed instantaneous streamwise velocity at a given instant are compared in figure 8(a) and (b). The reconstructed velocity contours clearly shows how effectively the POD is at filtering out the small scale eddies.

To better illustrate the dynamics of the coherent structures in the wall jet, the low-order reconstruction at several randomly selected instants are shown in figure 9. In this figure, the instantaneous streamwise velocity are shown in the first column and vector plots of the normal and lateral instantaneous velocity are shown in second column. In all cases, the mean has been added to the reconstructed velocity field. The instantaneous streamwise vorticity computed from these reconstructed velocities are shown in the third column.

The instantaneous streamwise velocity contours shown in figure 9(a) deviate significantly from the contours of the mean flow. The instantaneous results have a depression on the lower left side, near the wall and a bulging in the contours above that is caused by a large streamwise vortex [figure 9(b)] located on the left side of the flow that draws ambient fluid down and ejects it upward. Note that the magnitude of these fluctuations are approximately 60% of the maximum mean streamwise velocity. The contours of streamwise vorticity loosely correspond to these rotational flow regions.

Since the flow field acquired by the Stereo PIV system is not time resolved, it is very difficult to establish exact flow pattern/cycle, although similar behaviour can be observed at the other instants. Depressions in the contours of the streamwise velocity correspond to strong jets of fluid that are created by the presence of highly coherent streamwise vortex structures. These jets produce a rapid inflow of ambient fluid and are typically accompanied by strong lateral ejections of fluid [i.e. figure 9(m) and (p)]. Often these jets are oriented in pairs to cause a strong sweep of fluid across the entire lateral span of the jet [i.e. figure 9(v) and (y)]. This particular behaviour looks quite similar to the low-dimensional POD-Linear Stochastic Estimation reconstruction of the turbulent velocity field in the three-dimensional wall jet by Hall and Ewing (2010). In this case, the streamwise and lateral turbulent velocity field was estimated from time-resolved, POD filtered, spanwise fluctuating wall pressure measurements across the jet.

In all the reconstructions, a pair of oppositely signed regions of streamwise vorticity persists near the wall that are re-

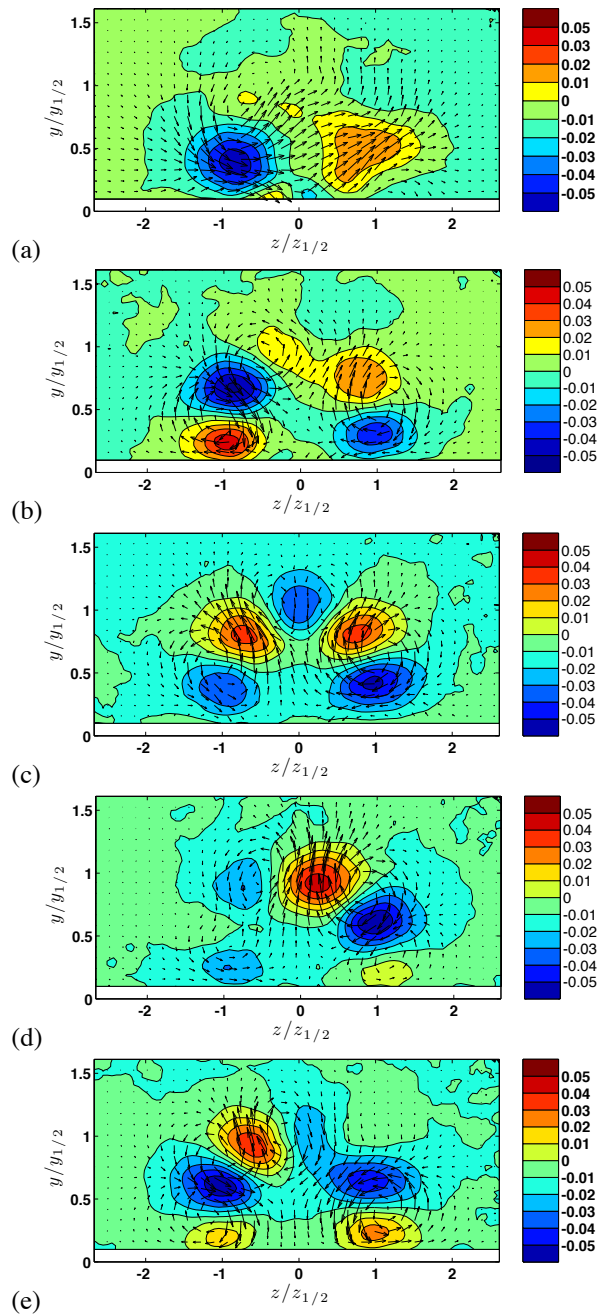


Figure 7. POD modes. (a) 1st mode, (b) 2nd mode, (c) 3rd mode, (d) 4th mode and (e) 5th mode.

markably similar to the contours of the mean streamwise vorticity (figure 5). These regions do not seem to be directly related to the regions of vorticity away from the wall. Inspection of the mean streamwise vorticity indicates that the streamwise vorticity regions away from the wall have no net contribution to the mean streamwise vorticity. Taken together, these results suggest that the streamwise vortex-structures formed in the jet outer shear-layers do not directly contribute to the mean secondary flow in the near-field of the three-dimensional wall jet. This is consistent with the findings of Hall and Ewing (2007b) who suggested that there were larger structures asso-

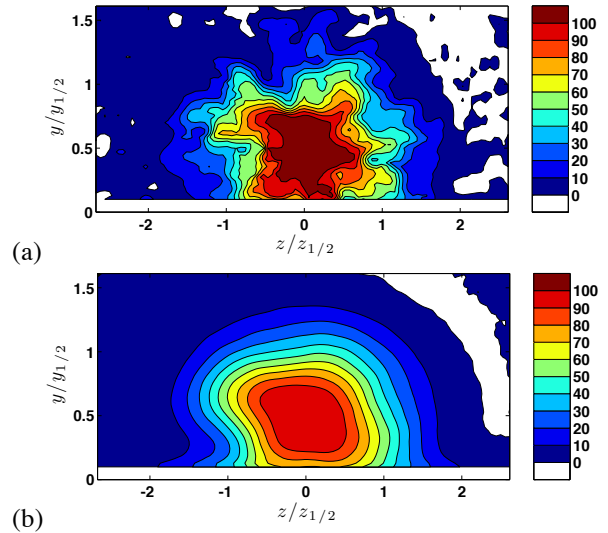


Figure 8. Contours of the instantaneous streamwise velocity. (a) Original, (b) Reconstructed using first five POD modes.

ciated with the outer layers and smaller faster moving structures located close to the wall at the center of the jet. These regions of near wall vorticity may be associated with these faster moving inner structures.

CONCLUDING REMARKS

The development of the three-dimensional wall jet was investigated using Stereoscopic PIV in the near-field region. The mean streamwise velocity contours are round with the exception of a bulging of the mean flow near the wall. This bulging is related to a mean lateral outflow of fluid near the wall at the centre of the jet and a mean lateral inflow of ambient fluid on the outside of the jet. This causes two regions of mean counter-rotating vorticity to be produced near the wall on either side of the lateral shear-layers.

To understand the underlying structures in the flow, the POD was performed on all 3 components of the turbulent velocity field. The reconstruction of the instantaneous flow velocity using the first five POD modes was found to be sufficient to deduce the features of the flow. The velocity reconstructions revealed that the distortion and bulging of the streamwise velocity contours was caused by strong jets of fluid induced by streamwise vortex structures in the outer shear-layers of the wall jet. The reconstructed instantaneous streamwise vorticity indicates the persistence of near wall regions of counter-rotating vorticity similar to the mean streamwise vorticity that seem to be independent of the vortex-structures in the outer shear-layer. This indicates that the coherent structures in the jet outer shear-layers do not directly contribute to the mean secondary flow in the jet, at least in the near-field.

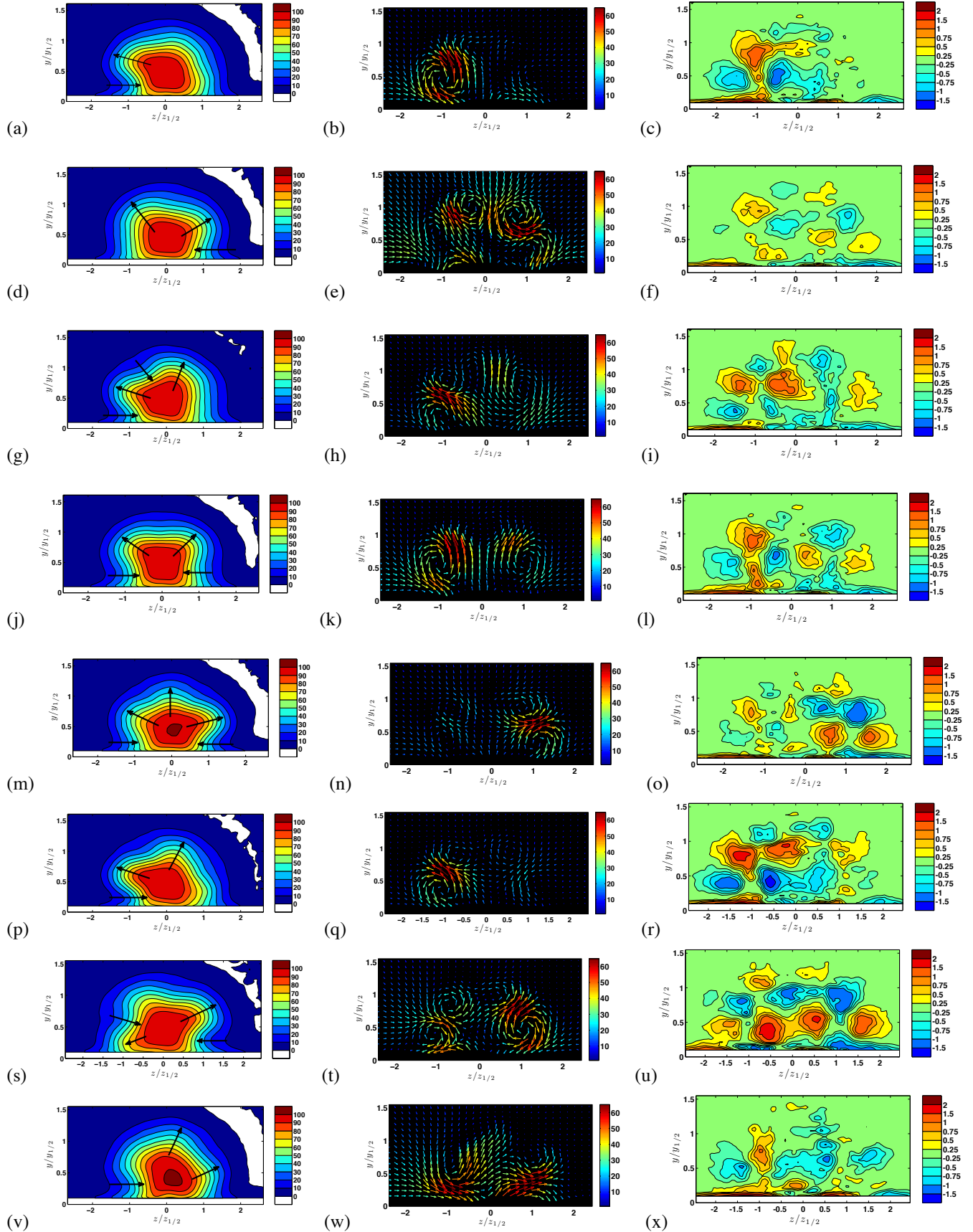
ACKNOWLEDGEMENTS

The authors are grateful for the financial support of NSERC.

Streamwise Velocity (U)

Vector Plots (V, W)

Streamwise Vorticity (Ω_x)



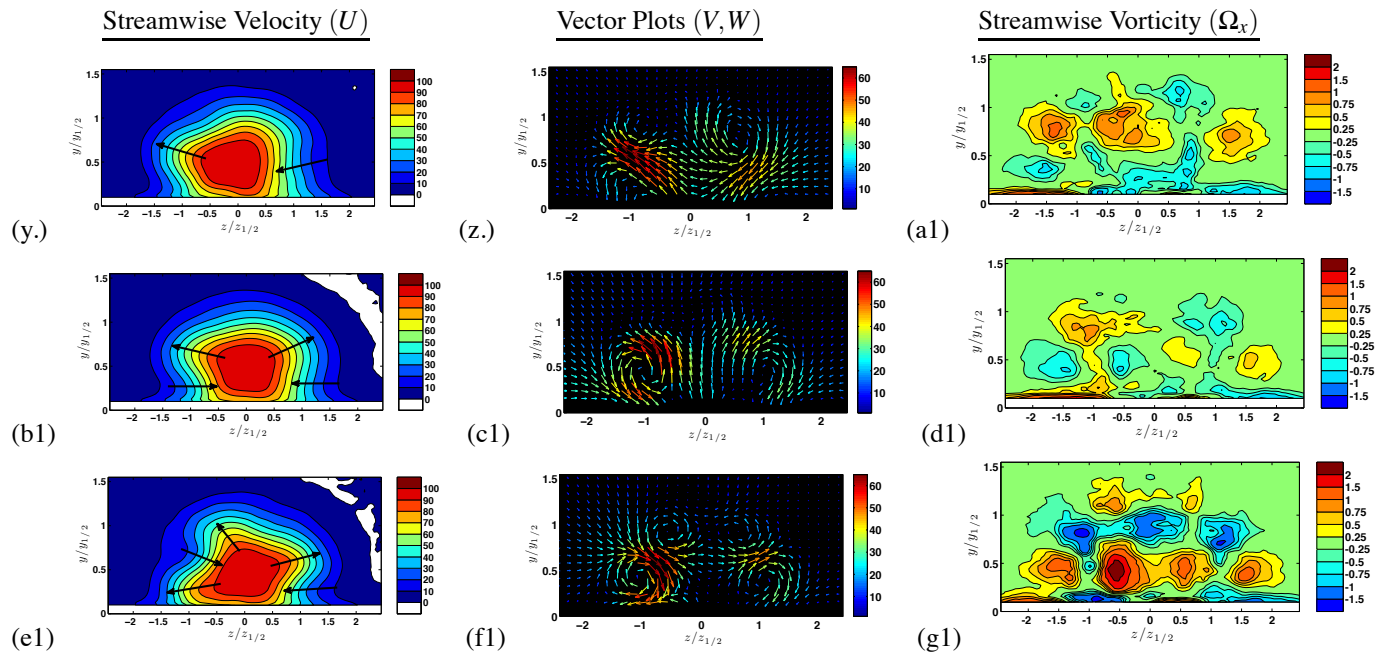


Figure 9. POD reconstruction of the instantaneous velocity using first five POD modes and reconstructed instantaneous streamwise vorticity.

REFERENCES

- M. Agelinchaab and M. F. Tachie. Characteristics of turbulent three-dimensional wall jets. *Journal of Fluids Engineering*, 133, 2011.
- J. H. Citriniti and W.K. George. Reconstruction of the global velocity field in the axisymmetric mixing layer utilizing the proper orthogonal decomposition. *Journal of Fluid Mechanics*, 418:137–166, 2000.
- T. J. Craft and B. E. Launder. On the spreading mechanism of the three-dimensional turbulent wall jet. *Journal of Fluid Mechanics*, 435:305–326, 2001.
- M. N. Glauser. *Coherent structures in the axisymmetric turbulent jet mixing layer*. PhD thesis, State University of New York at Buffalo, 1987.
- J. W. Hall and D. Ewing. The development of three-dimensional turbulent wall jets issuing from moderate aspect ratio rectangular channels. *AIAA Journal*, 45(6):1177–1186, 2007a.
- J. W. Hall and D. Ewing. The asymmetry of the large-scale structures in turbulent three-dimensional wall jets exiting long rectangular channels. *Journal of Fluids Engineering*, 129:929–941, 2007b.
- J. W. Hall and D. Ewing. Spectral linear stochastic estimation of the turbulent velocity in a square three-dimensional wall jet. *Journal of Fluids Engineering*, 132(5), 2010.
- B. E. Launder and W. Rodi. The turbulent wall jet measurements and modelling. *Annual Review of Fluid Mechanics*, 15:429–459, 1983.
- J. L. Lumley. The structure of inhomogeneous turbulent flow. In *Atmospheric Turbulence and Radio Wave Propagation*, pages 166–178, 1967.
- H. Matsuda, S. Iida, and M. Hayakawa. Coherent structures in three-dimensional wall jet. *Transactions of the ASME: Journal of Fluids Engineering*, 112:462–467, 1990.
- K. E. Meyer, J. M. Pedersen, and O. Ozcan. Turbulent jet in crossflow analysed with proper orthogonal decomposition. *Journal of Fluids Mechanics*, 583:199–227, 2007.
- L. Namgyal and J. W. Hall. PIV measurements of the turbulent secondary flow in a three-dimensional wall jet. In *Proceedings of ASME 2010 3rd Joint US–Engineering Summer Meeting & 8th International Conference on Nanochannels, Microchannels & Minichannels, Montreal, Canada, August 2010*. ASME. Paper Number FEDSM–ICNMM2010-30278.
- J. Pinier. *Low-dimensional Techniques for Active Control of High-speed Jet Aeroacoustics*. PhD thesis, Syracuse University, 2007.
- L. Sirovich. Turbulence and the dynamics of coherent structures. part i: Coherent structures. *Quarterly of Applied mathematics*, 45:561–571, 1987.
- H. Sun. *The effect of initial conditions on the development of the three-dimensional wall jet*. PhD thesis, McMaster University, Hamilton, Ontario, Canada, 2002.
- C. E. Tinney, M. N. Glauser, and L. S. Ukeiley. Low-dimensional characteristics of a transonic jet. part 1. proper orthogonal decomposition. *Journal of Fluid Mechanics*, 612:107–141, 2008.
- L. S. Ukeiley, L. Cordier, J. Delville, M. Glauser, and J. P. Bonnet. Examination of large-scale structures in turbulent plane mixing layer. *Journal of Fluid Mechanics*, 391:123, 1999.